

Article

Reaction with ROO• and HOO• Radicals of Honokiol-Related Neolignan Antioxidants

Nunzio Cardullo ¹, Filippo Monti ², Vera Muccilli ¹, Riccardo Amorati ^{3,*} and Andrea Baschieri ^{2,*}¹ Dipartimento di Scienze Chimiche, Università di Catania, V.le A. Doria 6, 95125 Catania, Italy² Istituto per la Sintesi Organica e la Fotoreattività (ISOF), Consiglio Nazionale delle Ricerche (CNR) Via Gobetti 101, 40129 Bologna, Italy³ Dipartimento di Chimica “G. Ciamician”, Università di Bologna, Via S. Giacomo 11, 40126 Bologna, Italy

* Correspondence: riccardo.amorati@unibo.it (R.A.); andrea.baschieri@isof.cnr.it (A.B.)

Abstract: Honokiol is a natural bisphenol neolignan present in the bark of *Magnolia officinalis*, whose extracts have been employed in oriental medicine to treat several disorders, showing a variety of biological properties, including antitumor activity, potentially related to radical scavenging. Six bisphenol neolignans with structural motifs related to the natural bioactive honokiol were synthesized. Their chain-breaking antioxidant activity was evaluated in the presence of peroxy (ROO•) and hydroperoxy (HOO•) radicals by both experimental and computational methods. Depending on the number and position of the hydroxyl and alkyl groups present on the molecules, these derivatives are more or less effective than the reference natural compound. The rate constant of the reaction with ROO• radicals for compound **7** is two orders of magnitude greater than that of honokiol. Moreover, for compounds displaying quinonic oxidized forms, we demonstrate that the addition of 1,4-cyclohexadiene, able to generate HOO• radicals, restores their antioxidant activity, because of the reducing capability of the HOO• radicals. The antioxidant activity of the oxidized compounds in combination with 1,4-cyclohexadiene is, in some cases, greater than that found for the starting compounds towards the peroxy radicals. This synergy can be applied to maximize the performances of these new bisphenol neolignans.

Keywords: antioxidant activity; honokiol; neolignans; peroxy radicals; hydroperoxy radicals; quinones' regeneration; radical reactions; reaction mechanisms; hydrogen atom transfer



Citation: Cardullo, N.; Monti, F.; Muccilli, V.; Amorati, R.; Baschieri, A. Reaction with ROO• and HOO• Radicals of Honokiol-Related Neolignan Antioxidants. *Molecules* **2023**, *28*, 735. <https://doi.org/10.3390/molecules28020735>

Academic Editor: Veronika Nagy

Received: 30 November 2022

Revised: 5 January 2023

Accepted: 7 January 2023

Published: 11 January 2023



Copyright: © 2023 by the authors. Licensee MDPI, Basel, Switzerland. This article is an open access article distributed under the terms and conditions of the Creative Commons Attribution (CC BY) license (<https://creativecommons.org/licenses/by/4.0/>).

1. Introduction

Lignans and neolignans are two groups of dimeric compounds widely distributed into the plant kingdom and biosynthesized through the shikimic acid pathway (Figure S1). The feature of these molecules is a peculiar dimeric structure originated by a β, β′-linkage between two phenyl propane units, C6C3, characterized by different degrees of oxidation in the side-chain and distinctive substituents occurring in the aromatic rings [1]. Their biosynthesis is originated from oxidative coupling involving phenyl propanoid units by enzymes such as laccase, peroxidase, or a cytochrome P450 [2], thus furnishing a wide range of dimeric compounds with different structures (Figure S1) [3]. For nomenclature purposes, the C6C3 units are treated as propylbenzene. When the linkage occurs between positions C-8 and C-8′ of two C6C3 units, the compound is a “lignan”; in a “neolignan”, the dimer is formed through a linkage involving two C6C3 units in positions different from C-8 and C-8′ (C-8-C5′, C-5-C-5′, etc.) [4]. In turn, given the high number of possible combinations, lignans are classified into eight groups according to structural patterns (Figure 1), whereas neolignans are classified into fifteen subgroups, indicated as NL1 to NL15 (Figure 2) [4].

Lignans and neolignans are polyphenols often studied for their antioxidant behavior [5]. Some non-exhaustive examples are in the following (Figure 3). Pinoresinol is one of the most representative lignans, found in sesame seeds and extra-virgin olive oil; it is

considered a high-value-added product with antioxidant activity, useful in chemoprevention [6]. (-)-Arctigenin is one of the main components of *Arctium lappa* whose extracts have been employed in Japanese Kampo medicine for antioxidant properties with benefits to human health [7]. A group of glucosidic dihydrobenzofuran neolignans have been also studied as antioxidants [8].

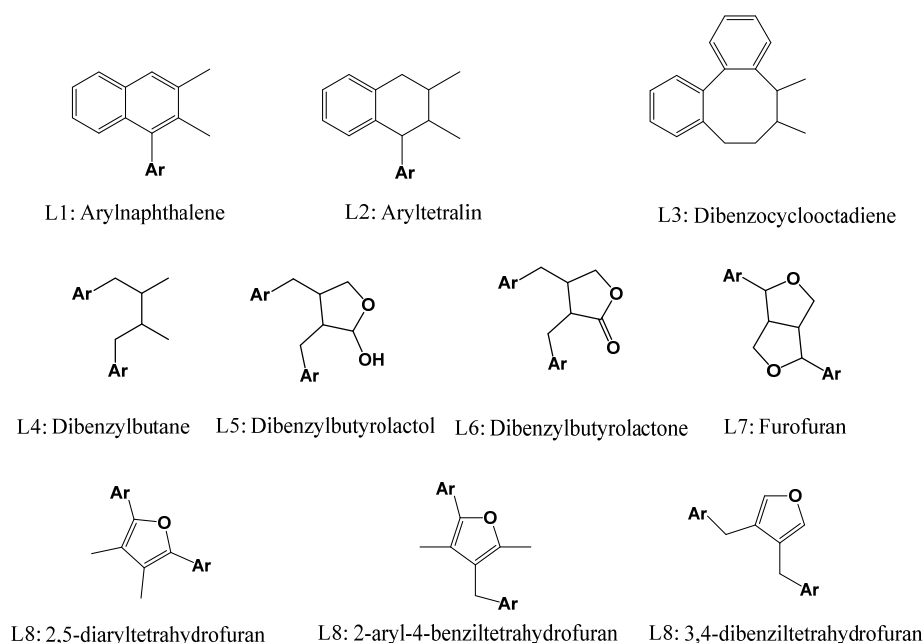


Figure 1. Classification of lignans according to Teponno et al. [4].

Magnolol and honokiol are neolignans with a diphenyl core (bisphenol neolignans, Figure 3); their structure is peculiar, and some authors consider the phenolic rings linked through a C–C bond a privileged structure which allows interaction with a variety of biological targets [9,10]. These two bisphenolic neolignans are present in the bark of *Magnolia officinalis* and other *M. spp*, whose extracts have been employed in oriental medicine to treat several disorders such as gastrointestinal disorders, anxiety, stress and allergic and cardiovascular diseases [11]. In addition to the antioxidant property, the two bisphenols have shown a number of biological properties, such as neuroprotective [12], antiviral [13], anti-inflammatory [14] and antitumor activities [15–17].

For this reason, recent works have been dedicated to the synthesis of new analogues inspired by magnolol and honokiol with the purpose of enhancing their biological activities [16,18–20].

In this frame, the antioxidant behavior of magnolol and its isomer honokiol (**1**) has been deeply studied [21–23]. Interestingly, the two compounds have shown different antioxidant profiles derived from the position of the OH groups. In organic solvents, magnolol was more active as a peroxy ($\text{ROO}\bullet$) radical quencher than honokiol, because of the stabilization of the phenoxy radical by an intramolecular H-bond [23]. Indeed, the study of the kinetics of $\text{ROO}\bullet$ and $\text{HOO}\bullet$ radical trapping is of great relevance because these radicals are responsible for the propagation of the oxidative chain during lipid peroxidation [24], and are implicated in important biochemical processes such as ferroptosis [25].

The synthesis of bioinspired natural antioxidants represents a strategy to gain new molecules showing stronger antioxidant capacity than natural leads. A similar or even better antioxidant profile has been observed for bioinspired derivatives of magnolol as measured by the rate constant of the reaction with $\text{ROO}\bullet$ radicals [26]. As a continuation of these investigations, six bisphenol neolignans with structural features resembling the natural bioactive honokiol (**1**) were synthesized and evaluated for their antioxidant behavior (Figure 4). In particular, we have designed honokiol-related compounds **2** and **3** to compare their antioxidant profiles with that of **1** and to understand a possible role in the oxidative

processes arising from the presence of the ortho-allyl chain. Furthermore, supposing **2** and **3** will result in promising antioxidants, the presence of the 2-hydroxyethyl chain in *para* position to OH could allow the insertion of other functional groups to gain compounds with different physicochemical properties for future studies. Moreover, in a previous work, the bisphenol **8** (3,3',5,5'-tetramethyl-[1,1'-biphenyl]-4,4'-diol) has shown a large rate constant for reaction with peroxy radicals, arising from the conjugation of the radical on both aromatic rings, and from the presence of the methyl groups in the ortho position that reduce the bond dissociation enthalpy of OH. In addition, this compound showed a stoichiometric coefficient of 1.9 in the autoxidation of styrene, indicating that it transfers the second O–H atom to a second peroxy radical. Based on these findings, we have designed bisphenols **5** and **6** and thus catechol **7** and its methylated analogue **4**. The kinetics of peroxy and hydroperoxy radical trapping was studied using the inhibited autoxidation method which provides, with respect to other simplified methods based on the decay of colored radicals, a more solid prediction of efficacy in real conditions [27].

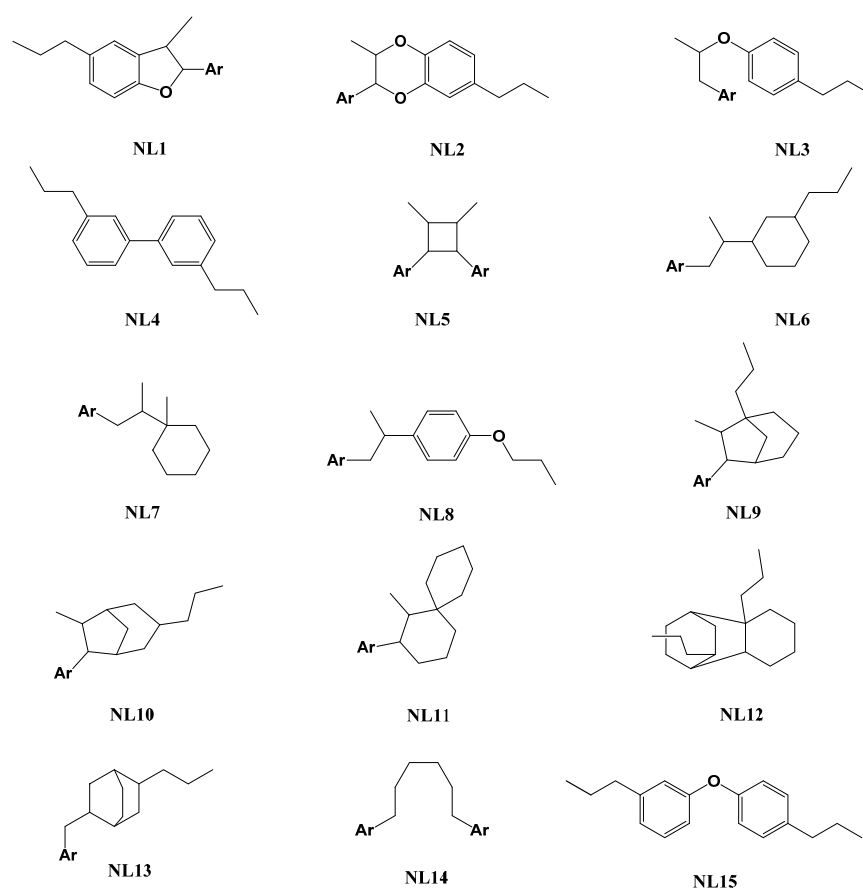


Figure 2. Classification of neolignans according to Teponno et al. [4].

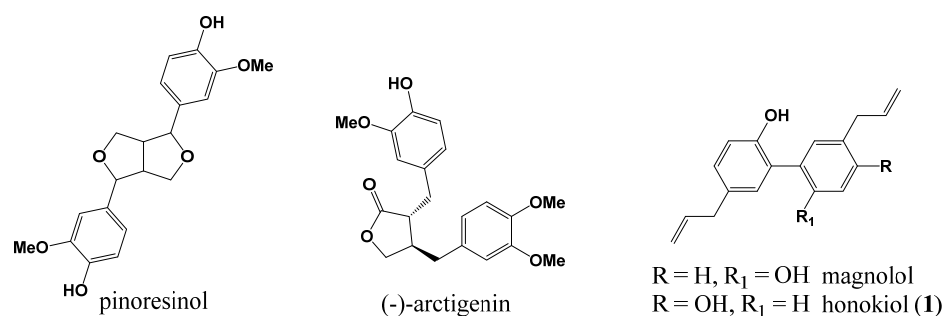


Figure 3. Structure of pinoresinol, arctigenin, magnolol and honokiol (**1**).

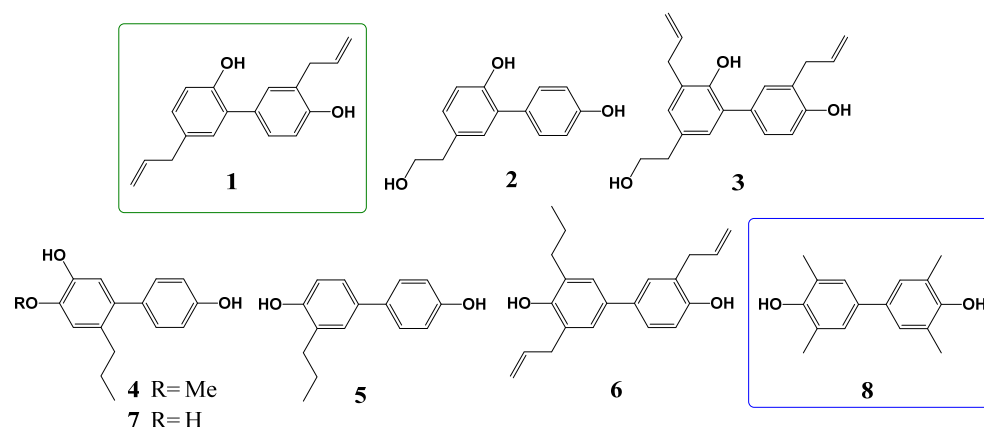
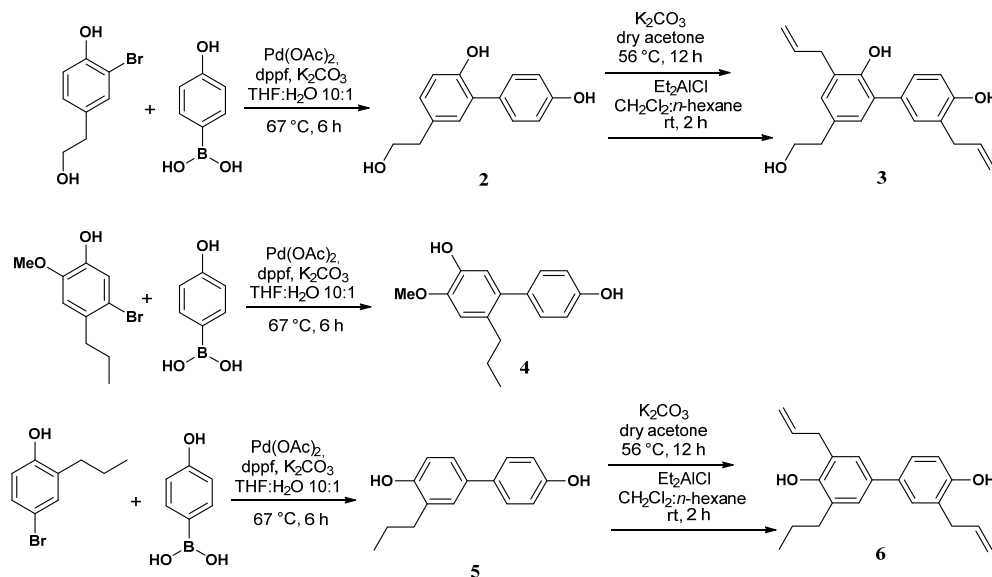


Figure 4. Antioxidants investigated in this study. Honokiol (1) and other bisphenol neolignans 2–7. Compound 8 was previously studied [23]. It is here reported to highlight the structural analogy with compounds 4–7.

2. Results and Discussion

2.1. Synthesis of Bisphenol Neolignans 2–7

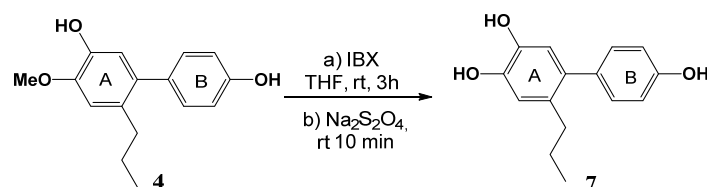
Bisphenol neolignans 2–6 were synthesized following a previously described strategy [28] based on a Suzuki–Miyaura cross-coupling step between a suitable aryl halide and 4-hydroxy-phenyl boronic acid, to build the biphenyl skeleton of compounds 2, 4 and 5. Subsequently, S_N2 reaction in presence of allyl bromide followed by Claisen rearrangement in mild conditions allowed us to isolate the C-allyl derivatives 3 and 6. The spectroscopic data of these compounds are in agreement with those previously reported [28] (Scheme 1).



Scheme 1. Synthesis of bisphenol neolignans inspired by honokiol.

On the contrary, the synthesis of catechol 7 is reported herein for the first time. As depicted in Scheme 2, the bisphenol 4, obtained by Suzuki coupling, was converted into the catechol analogue employing hypervalent-iodine chemistry, according to literature reports on similar substrates [16,26,29]. In particular, 2-iodoxybenzoic acid (IBX) was prepared following the protocol of Frigerio M. et al. [30]. IBX was employed in slight excess with respect to 4 (1.2 equiv) and in THF. These represent the optimal conditions to gain the oxidative demethylation of a guaiacol group, thus achieving the bis-*ortho*-quinone intermediate which is converted into the final catechol when a saturated $\text{Na}_2\text{S}_2\text{O}_4$ solution is added to the mixture. The compound was isolated after column chromatography with

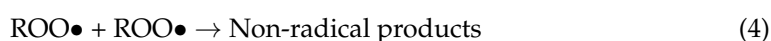
a 38% yield. Details and spectroscopic data (NMR and MS data) of the new bisphenol 7 are reported in the Materials and Methods section. Notably, IBX is more environmentally friendly, if compared with other oxidizing agents based on heavy or toxic metals and/or requiring strong reaction conditions.



Scheme 2. Synthesis of catechol neolignan 7.

2.2. Kinetics and Stoichiometry of the Reaction with Peroxyl Radicals

The antioxidant activity of honokiol (1) and six inspired bisphenol neolignans 2–7 (AH) was evaluated by measuring the rate constant (k_{inh}) for the reaction with peroxyl radicals ($ROO\bullet$) that are responsible for oxidative chain propagation in many natural materials [31].



where, R_i is the rate of initiation (reaction 1). Equations (1)–(4) represent the autoxidation of substrate RH in the absence of antioxidants, while Equations (5) and (6) represent chain-breaking inhibition by antioxidant AH.

The inhibition rate constants (k_{inh}) of antioxidants 1–7 (i.e., the rate constant of reaction 5), were determined by studying the inhibition of the thermally initiated autoxidation of cumene or styrene (RH) under controlled conditions using chlorobenzene or acetonitrile as the solvent [32].

All reactions were performed at 303 K using 2,2'-azobis(isobutyronitrile) (AIBN) as initiator and were followed by monitoring the oxygen consumption in an oxygen uptake apparatus based on a differential pressure transducer [27,32].

For the very first step, the rate of radical initiation produced by AIBN (R_i) was determined in matched preliminary experiments using the inhibitor method, according to Equation (7)

$$R_i = n [AH]/\tau \quad (7)$$

where τ is the length of the inhibition time. Tocopherol's mimic 2,2,5,7,8-pentamethyl-6-chromanol (PMHC) was used as reference antioxidant, with $n = 2$.

In the presence of effective antioxidants, substrate oxidation and oxygen consumption are much slower and a clear inhibition period is observed, as shown in Figure 5.

The rate constant for the reaction between $ROO\bullet$ radicals and 1–7 could be obtained from the rate of O_2 consumption (the slope of the oxygen consumption) during the inhibited period from the known constants k_p and $2k_t$ for cumene (and styrene) chain propagation and termination, respectively, using Equation (8) where R_{ox0} and R_{ox} represent the O_2 consumption rate in the absence and in the presence of the antioxidant, respectively (see Experimental Section and ref [32–36] for more explanations).

$$\frac{R_{ox0}}{R_{ox}} - \frac{R_{ox}}{R_{ox0}} = \frac{nk_{inh}[AH]_0}{\sqrt{2k_tR_i}} \quad (8)$$

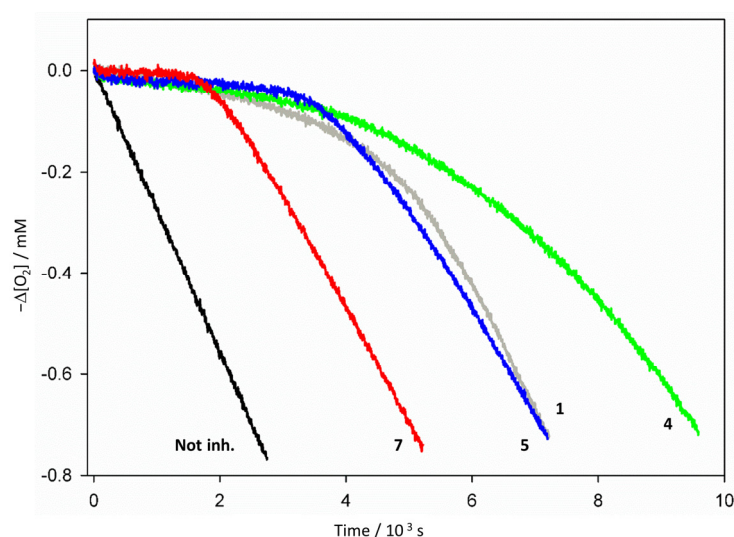


Figure 5. Selected examples of oxygen consumption during the autoxidation of Cumene (3.6 M) initiated by AIBN (0.05 M) in PhCl at 30 °C without inhibitors (black) or in the presence of antioxidant (0.7×10^{-5} M) 7 (red) and (1.4×10^{-5} M) 5 (blue), 1 (grey), 4 (green).

The stoichiometric coefficient n , which represents the number of ROO• radicals trapped by each antioxidant molecule, is instead determined from the duration of the antioxidant effect. The values of k_{inh} and n , determined in chlorobenzene and acetonitrile, are reported in Table 1.

Table 1. Rate constants for the reaction with peroxy radicals in chlorobenzene or acetonitrile at 303 K, and number of trapped radicals (n)^{1,2}.

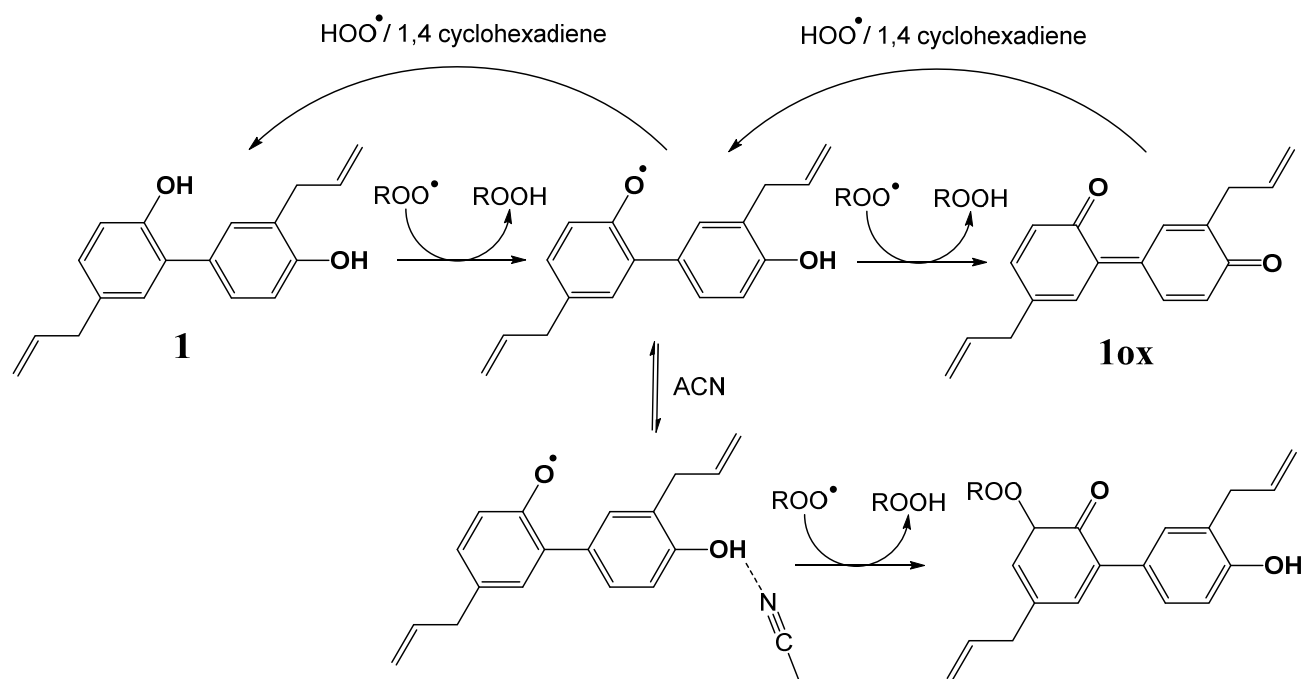
Sample	Chlorobenzene		Acetonitrile		KSE ³
	$k_{\text{inh}} / \text{M}^{-1}\text{s}^{-1}$	n	$k_{\text{inh}} / \text{M}^{-1}\text{s}^{-1}$	n	
1	$(1.2 \pm 0.2) \times 10^4$	2.3 ± 0.2	$(8.2 \pm 0.3) \times 10^3$	3.5 ± 0.5	1.5
2	$(6.7 \pm 0.3) \times 10^3$	1.9 ± 0.1	$(3.2 \pm 0.2) \times 10^3$	2.4 ± 0.4	2.1
3	$(6.1 \pm 0.4) \times 10^3$	1.9 ± 0.1	$(4.0 \pm 0.4) \times 10^3$	2.1 ± 0.2	1.5
4	$(1.1 \pm 0.2) \times 10^4$ first OH $(2.3 \pm 0.4) \times 10^3$ s OH	3.8 ± 0.3	$(5.6 \pm 0.3) \times 10^3$	2.6 ± 0.4	2.0
5	$(2.5 \pm 0.2) \times 10^4$	2.0 ± 0.1	$(7.6 \pm 0.3) \times 10^3$	2.1 ± 0.1	3.3
6	$(1.5 \pm 0.2) \times 10^4$	1.8 ± 0.2	$(1.0 \pm 0.3) \times 10^4$	2.1 ± 0.1	1.5
7 ⁵	$(1.2 \pm 0.1) \times 10^6$	2.0 ± 0.1	$(2.5 \pm 0.2) \times 10^4$	2.0 ± 0.1	48

¹ From cumene autoxidation studies unless otherwise noted. ² All values are average from at least 3 independent measurements. Errors for n and k_{inh} represent \pm SD. ³ Kinetic Solvent Effect, defined as $KSE = k_{\text{inh}}(\text{PhCl}) / k_{\text{inh}}(\text{MeCN})$. ⁴ Relatives for the first reactive OH group. ⁵ Measured in styrene.

To fully solubilize the samples, 0.2% (*v/v*) methanol was added to all chlorobenzene and in acetonitrile solutions. For this reason, it was also necessary to re-evaluate, even if already reported in the literature [23], the rate constants of honokiol 1, since it was used as a reference compound for all the other investigated molecules. Despite being present in a very small amount, methanol strongly affects the inhibition constant of honokiol 1 in chlorobenzene by decreasing it about three times (see Table 1 vs. ref [23]). Conversely, in acetonitrile, this effect is limited, since such solvent already forms hydrogen bonds with the OH groups of the antioxidant molecules. Additionally, in this series of experiments, the number of radicals trapped by honokiol 1 in chlorobenzene is equal to 2, while it nearly doubles in acetonitrile.

In PhCl, as previously demonstrated, the phenoxyl radical from honokiol 1 reacts with a second ROO• radical by formal H-atom transfer from an OH group, leading to the formation of the corresponding dienone 10x (Scheme 3). In MeCN, on the other hand, the

second OH group in the phenoxyl radical from honokiol **1** is H-bonded to the solvent, and therefore it is less available to be transferred to a second ROO• radical, as shown in Scheme 3. As a consequence, the phenoxyl radical decays preferably through the addition of a second ROO• radical to the aromatic ring. The intact second phenolic ring is then available to trap two additional peroxy radicals, similarly to monophenolic compounds but with a lower k_{inh} than the first OH, presumably because of the unfavourable electronic effect of the oxidized ring.

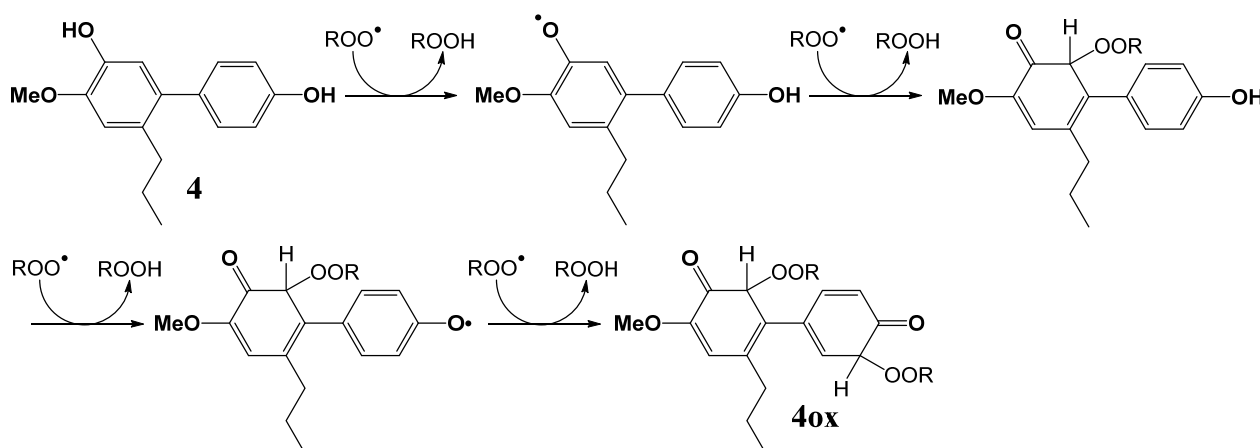


Scheme 3. Mechanism showing the peroxy-radical trapping by honokiol **1** in chlorobenzene (stoichiometric coefficient = 2) and for the antioxidant synergy between 1,4 cyclohexadiene and polyphenolic antioxidants (**Top**); proposed change in the stoichiometric coefficient ($n = 4$) in acetonitrile due to the H-bonding between the intermediate phenoxyl radical of **1** and the solvent (**Bottom**).

Antioxidants **2** and **3** are comparable to **1**. The inhibition constant is about half that of honokiol both in a non-polar solvent, such as PhCl, and in a polar solvent, such as MeCN. In compound **2**, the absence of alkyl groups lowers the stability of the phenoxyl radical intermediate, while electronegative O-atom in the hydroxyethyl chain has a small negative impact on the inhibition constant. In compound **3**, the allyl substituent present in an *ortho* position with respect to the -OH groups limits the H-atoms abstraction because of a OH— π interaction, as previously reported [23].

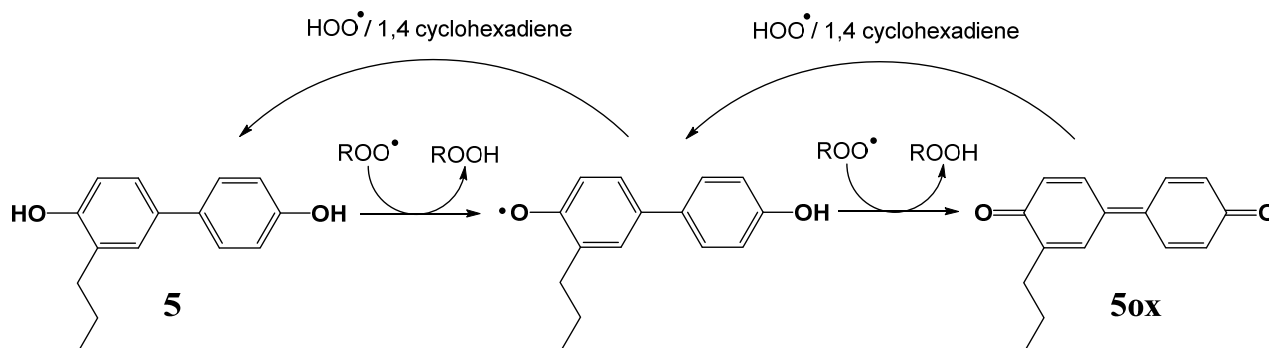
The number of radicals trapped by these last two compounds is the same as for the reference compound **1**. In MeCN, for the second phenolic ring, the stoichiometric coefficient could not be measured because the k_{inh} value is too low. For this reason, we only found $n = 2$.

Compound **4** has a different structure than honokiol. Due to the different position of a phenolic group in one of the two rings, it is not possible to obtain the corresponding quinonic form and therefore the two phenolic rings can be considered independent. Each ring traps 2 radicals with the addition of the peroxy radical (Scheme 4). The inhibition constant of the more reactive -OH group is completely comparable to that of compound **1**, while the second constant is about 10 times lower. For this reason, only the first can be observed and measured in MeCN.



Scheme 4. Mechanism for the trapping of peroxy radicals by compound 4 in chlorobenzene (stoichiometric coefficient = 4, experimental $n = 3.8$).

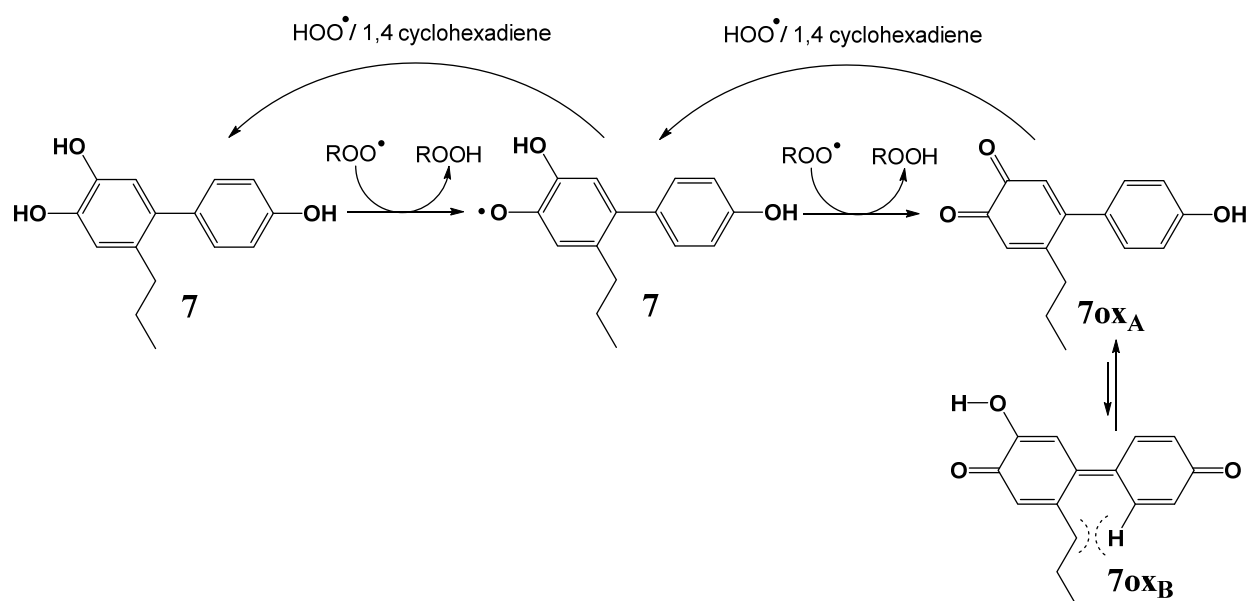
Bisphenols **5** and **6** display relatively large k_{inh} values compared to honokiol, with the k_{inh} of **5** being about twice that of **6**. As already demonstrated for compound **3**, the presence of allyl substituents reduces the antioxidant activity of these compounds, due to hydrogen bonding between allylic and hydroxyl groups; such an effect is less noticeable in a polar solvent such as MeCN [23]. Since both **5** and **6** have a stoichiometric coefficient of about 2 in the inhibited autoxidation of cumene, it is expected that the phenoxyl radicals from both **5** and **6** transfer the second O–H atom to another peroxy radical, as shown in Scheme 5.



Scheme 5. Mechanism for the trapping of peroxy radicals by compounds **5** in chlorobenzene (stoichiometric coefficient = 2) and for the antioxidant synergy between 1,4 cyclohexadiene and polyphenolic antioxidants.

The inhibition shown by compound **7** is the highest of all the investigated compounds, as expected from the presence of a second OH group in *ortho*-position (catechol moiety) (Scheme 6). In this case, the experiments were performed in styrene. Styrene is typically employed for studying strong antioxidants (i.e., with $k_{inh} > 1 \times 10^5 \text{ M}^{-1}\text{s}^{-1}$), whereas cumene, thanks to its low k_p and $2k_t$ values, is suitable for weaker inhibitors [32]. The k_{inh} of **7** is two orders of magnitude greater than compounds **1–6**, but it corresponds to the trapping of only two $\text{ROO}\bullet$ radicals.

This behaviour is reminiscent of that observed in *ortho*-bisphenol derivatives [37,38]. It can be explained by considering that, after the trapping of the first two $\text{ROO}\bullet$ radicals, one of the two phenolic rings is converted into the corresponding *ortho*-benzoquinone, which has an unfavourable effect on the second phenolic ring, reducing its reactivity, possibly because of electron-withdrawing effect. In our case, the *ortho*-quinonic form **7ox_A** is also in equilibrium with the dienonic form **7ox_B**.



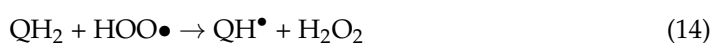
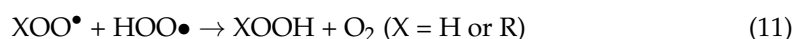
Scheme 6. Mechanism for the trapping of peroxy radicals by catechol derivative **7** in chlorobenzene (stoichiometric coefficient = 2) and for the antioxidant synergy between 1,4 cyclohexadiene and polyphenolic antioxidants. Theoretical calculations predict that tautomer **7ox_A** is more stable than **7ox_B** by 7.1 kcal/mol.

As shown in Table 1, the k_{inh} values decrease for all phenols when the polarity of the solvent is increased (i.e., in acetonitrile); this is known as the kinetic solvent effect (KSE), which occurs in case of H-atom abstraction from polar X–H bonds [39]. The decrease is more evident for **7**, as the KSE is 48, while it ranges from 1 to 3 for compounds **1–6**. Notably, this phenomenon has already been studied for other compounds having a catechol ring [40,41]. The solvent engages in H-bonds with phenolic OH groups, and decreases their reactivity towards the peroxy radicals by preventing the formation of the H-atom transfer pre-reaction complex. As for the other compounds, the lowest values (about 1.5) are observed in molecules equipped with allyl groups. Indeed, such groups, already form H-bonds with hydroxyl groups, so the effect in MeCN is less evident. Accordingly, slightly higher values (about 2 or 3), are found for compounds having unsubstituted phenolic rings.

2.3. Hydrogen Atom Transfer from HOO• to Quinones

As described above, with the exception of compound **4**, the honokiol-inspired bisphenol neolignans, upon reaction with the peroxy radicals in chlorobenzene, oxidize to the corresponding quinone forms **1ox**, **5ox** and **7ox** (see Schemes 3–6).

Autoxidation of 1,4 cyclohexadiene (CHD) to benzene is a well-known chain process, in which HOO• acts as a propagating radical (Equation (10)) [42,43].



Equations (12)–(15) explain the key reactions of the antioxidant activity of quinones, ($Q = 1\text{ox}$, 5ox and 7ox), in the presence of 1,4-cyclohexadiene.

The addition of CHD in the peroxidation of oxidizable substrates (RH) partially changes the propagation chain-carrier from $\text{ROO}\bullet$ to $\text{HOO}\bullet$ (hydroperoxyl radical) since CHD itself is rapidly attacked by $\text{ROO}\bullet$ and releases $\text{HOO}\bullet$. Such hydroperoxyl radicals can both propagate the oxidation reaction or be quenched by another $\text{HOO}\bullet$ or by a $\text{ROO}\bullet$ radical (self-termination or cross-termination).

To achieve a better understanding of the regeneration mechanism of phenolic antioxidants by CHD, experiments were conducted by injecting CHD 26 mM into the styrene autoxidation system after the phenolic antioxidant was consumed at the time that the substrate starts to oxidize again and approximately the whole compound is in the form of an oxidized product.

As shown in Figure 6D, the injection of CHD into the reaction, when sample 4 has been completely oxidized, provides only a very small increase in the inhibition (Figure 6D and Table 2).

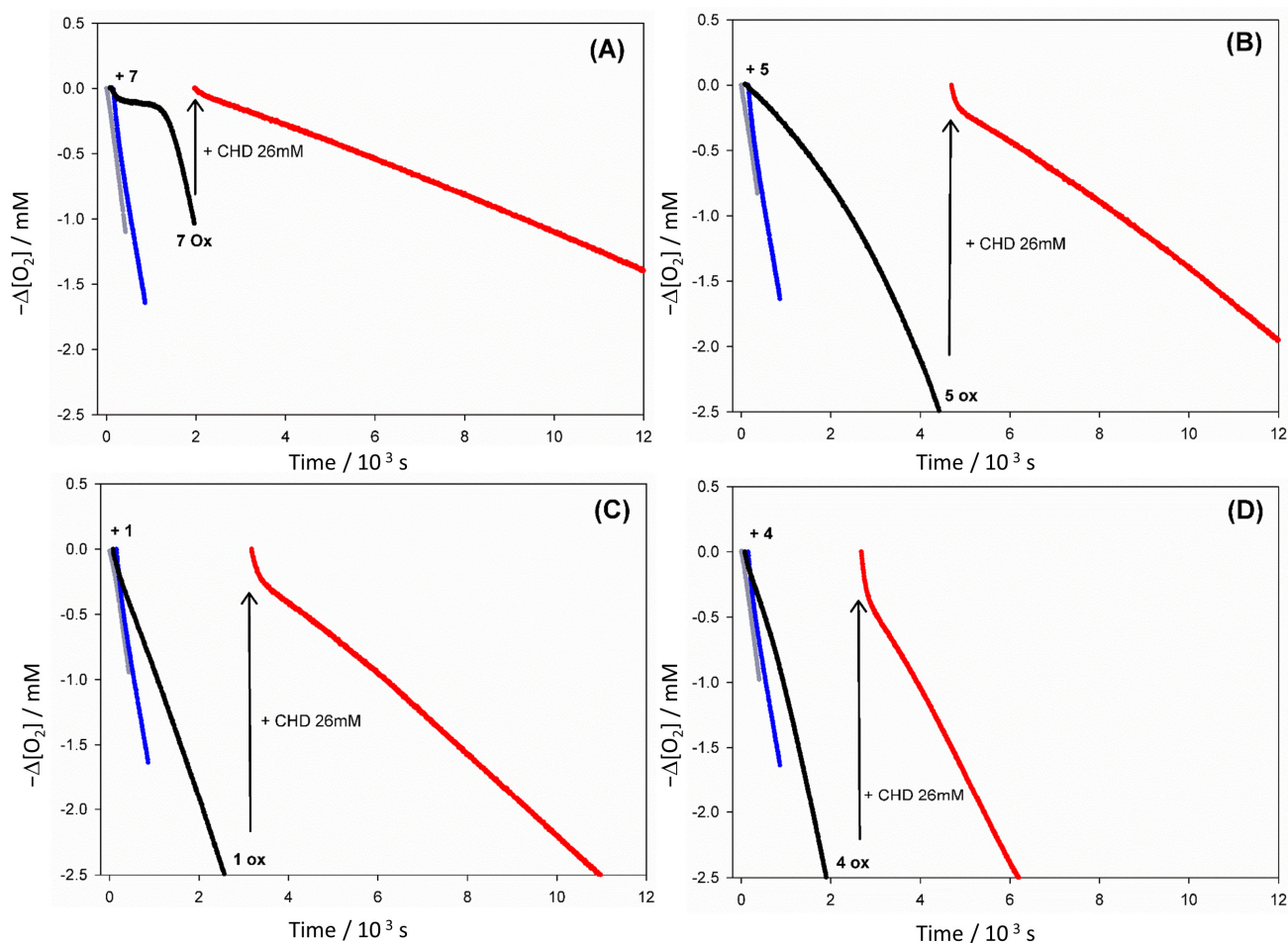


Figure 6. Oxygen consumption during the autoxidation of styrene (4.3 M) initiated by AIBN (0.05 M) in PhCl at 30 °C; without inhibitors (grey) or in the presence of 1,4 cyclohexadiene 26 mM (blue) or in the presence of (panel A) antioxidant 7 10 μM ; (panel B) antioxidant 5 13 μM ; (panel C) antioxidant 1 13 μM ; (panel D) antioxidant 4 13 μM (black) and the subsequent injection of 1,4 cyclohexadiene 26 mM (red).

On the other hand, in the presence of fully exhausted honokiol 1 or compounds 5 or 7, the addition of CHD triggers a new inhibition period (Figure 6A–C and Table 2). We explain this effect by considering that the quinones formed as the final oxidized products ($Q = 1\text{ox}$, 5ox and 7ox) can be reduced back to the starting antioxidant, confirming the

mechanism suggested in Schemes 3–6. When catechols behave as antioxidants, quinones are easily formed upon oxidation and they are generally expected to be their final oxidized products. Although such a mechanism is less obvious for other polyphenolic compounds, we were able to demonstrate the formation of the corresponding quinones also for honokiol and the bisphenol 5. Comparing the kinetic traces in Figure 6, we should notice that the rate of O₂ uptake during the inhibition period is smaller for 7 than for 1 and 5, demonstrating the superior antioxidant activity of the *ortho*-isomer (Table 2).

Table 2. Regeneration effect of CHD on quinones and reactivation of their antioxidant activity.

Sample	Slope A ¹ without Inhibitors + 26 mM CHD $d[\text{O}_2]/dt$ (μMs^{-1})	Slope B Oxidized Form + 26 mM CHD $d[\text{O}_2]/dt$ (μMs^{-1})	Slope Reduction A/B
7		0.123	16.3
5	2.0 ± 0.2	0.227	8.8
1		0.271	7.4
4		0.657	3.0

¹ Rate of oxygen consumption during the autoxidation of styrene (4.3 M) initiated by AIBN (0.05 M) in PhCl at 30 °C.

The reduction of all quinones is attributed to the release of HOO• during the autoxidation of CHD which acts as the reducing agent. This uncommon reducing behavior might be counterintuitive for a reputedly oxidizing radical, but it is supported by previous solid evidence [44–46].

From the slopes shown in Figure 6 (red lines vs. black lines), it is clear that the antioxidant effect of 1, 5 and 7 is visibly lower than that of oxidized products 1ox, 5ox and 7ox with CHD, except for compound 7 and its product, which are both high. Additionally, the inhibition length is clearly higher when HOO• radicals produced by the co-oxidation of CHD with styrene are present in the reaction environment.

Therefore, quinones formed by oxidation of 1, 5 and 7 are effectively regenerated by HOO• radicals; this synergic antioxidant chemistry, exploiting CHD in combination with polyphenolic compounds, is more effective than traditional antioxidant systems.

2.4. Theoretical Calculation of Bond Dissociation Enthalpies

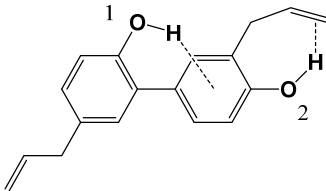
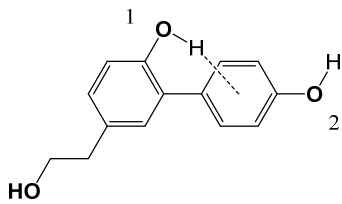
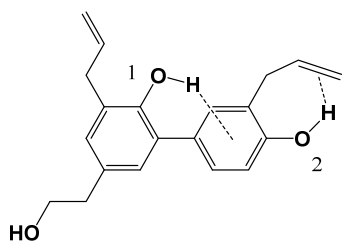
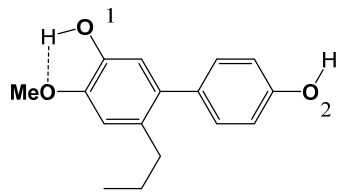
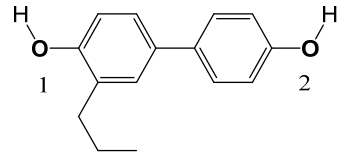
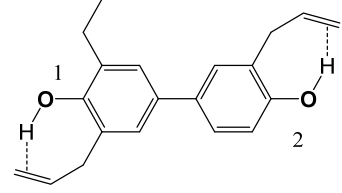
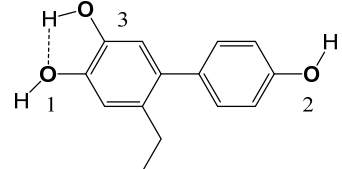
To rationalize the kinetic results, the preferred conformations and the dissociation enthalpies of the O–H bonds (BDE(OH)) were computed by DFT methods at the B3LYP-D3/6-31+G(d,p) level [47–50], using the SMD [51] implicit solvation model, as implemented in the Gaussian 09 [52]. The BDE(OH) values in chlorobenzene were obtained by using an isodesmic approach that consists of calculating the BDE difference between the investigated compounds and phenol ($\Delta\text{BDE}(\text{OH})$), and by adding this value to the known experimental BDE(OH) of phenol in benzene (86.7 kcal/mol) (Equation (16)).

$$\text{BDE}(\text{OH}) = 86.7 + \Delta\text{BDE}(\text{OH}) \quad (16)$$

The results of BDE(OH) calculations for both the hydroxyl groups present in compounds 1–7 are shown in Table 3. From these calculations, it is possible to recognize which phenolic ring is intrinsically more reactive towards peroxy radicals, allowing us to know the structure of the corresponding semiquinone that is generated. While BDE(OH) alone is not a complete descriptor of k_{inh} , nevertheless, for phenols having similar steric crowding around the reactive OH, a Evans-Polanyi-type relationship between $\text{Log}(k_{\text{inh}})$ and BDE(OH) can be observed.

In the case of compounds 1–7, the fairly linear relationship (Figure 7) indicates that theoretical calculations account with reasonable accuracy the reactivity of ROO• radicals in non-polar media and confirms the previous structure–activity relationship discussion for the compounds studied in this manuscript.

Table 3. O–H bond dissociation enthalpies for the investigated phenols.

	Compound	BDE(OH)/kcal/mol	
		1-OH	2-OH
1		83.6	85.1
2		83.8	85.3
3		83.2	85.8
4		82.8	84.2
5		81.5	82.5
6		81.9	83.0
7		77.0	84.3

The bond dissociation enthalpy of the O–H bond of semiquinones **10x**, **50x** and **70x** was also calculated by DFT methods to confirm their reactivity towards hydroperoxyl radicals as observed in previous experiments, in the presence of CHD. The reaction of semiquinones with $\text{HOO}\bullet$ depends on the BDE of the phenolic O–H bond in the semiquinone. If the BDE is high, the quinone will react more easily with hydroperoxyl radicals and there will be an overall antioxidant effect on the system.

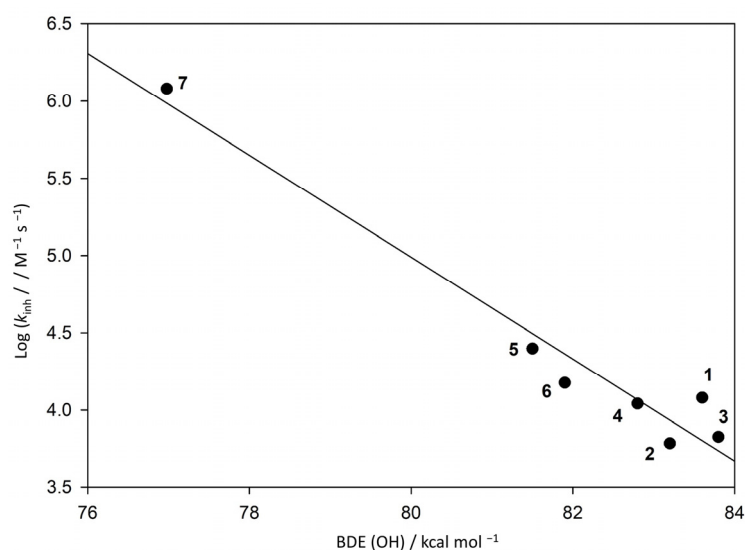


Figure 7. Relationship between experimental inhibition constant and theoretical BDE(OH).

It is known that the semiquinone obtained from the reaction of 2,5-di-*tert*-butylhydroquinone with peroxy radicals is able to react with molecular oxygen, dissolved in air-equilibrated solutions [53]. For this reason, the BDE(OH) of 1,4-semiquinone was calculated and used as a reference (65.3 kcal/mol). The semiquinones of compounds **1ox**, **5ox** and **7ox** have BDE(OH) values of 79.2, 75.2 and 73.6 kcal/mol, respectively. Since these values are greater than the BDE of 1,4-semiquinone, the quinones **1ox**, **5ox** and **7ox** are expected to have a fast reaction with HOO• radicals, while having a slow reverse reaction of the corresponding semiquinone with oxygen. The BDE(OH) order would predict that HOO• trapping decreases in the order **1ox** < **5ox** < **7ox** << 1,4-benzoquinone. However, these BDE values, obtained by DFT methods, are only a theoretical prediction of the synergistic effect between CHD and the oxidized products; this does not take into account kinetic aspects, such as the stability in solution of these quinones, and the formation of a non-regenerable products obtained by adding peroxy radicals to the phenolic rings, which have the effect of reducing the concentration of quinone available for the reaction with HOO•. Nevertheless, the comparison between the data obtained with DFT methods and those obtained in the above experiments fully rationalize the obtained results and confirm the proposed reaction mechanisms.

3. Materials and Methods

3.1. Materials

All chemicals were of reagent grade and were used without further purification. Where necessary, starting materials, namely aryl halides [28] IBX were freshly prepared as previously described [30]. Solvents were of the highest grade commercially available and were used as received. Commercially available honokiol **1** was purchased from TCI Europe (Milan, Italy), PMHC (2,2,5,7,8-Pentamethyl-6-chromanol) and AIBN were purchased from Sigma-Aldrich (Milan, Italy). Cumene, styrene and 1,4 cyclohexadiene were purified by double percolation through silica and activated alumina columns before use. AIBN was recrystallized from methanol and stored at $-18\text{ }^{\circ}\text{C}$.

NMR spectra were acquired on a Varian Unity Inova spectrometer (Italy, Milan) operating at 499.86 (^1H) and 125.70 MHz (^{13}C). 1D and 2D NMR experiments (gHSQC, and gHMBC) were performed at 300 K. A high-resolution MS spectrum of **7** was run on a Q Exactive Orbitrap mass spectrometer (Thermo Fisher Scientific, Bremen, Germany) equipped with an ESI ion source operating in negative ion mode. Compound **7** was directly infused in the spectrometer, and a survey scan was performed from m/z 150 to 1000 at 140 k resolution.

3.2. Synthesis of Bisphenol Neolignans

Compounds 2–6, used in the present investigation, were synthesized as described previously and as depicted in Scheme 1 [28].

Compound 7 was synthesized for the first time as reported in the following. The purity of these compounds was verified by ^1H NMR analysis.

The bisphenol 4 (62.6 mg, 0.24 mmol) was solubilized in THF (4 mL) and IBX (80.2 mg, 1.2 equiv.) was added under stirring to the solution. The mixture was stirred at rt for 3 h. Then, a saturated $\text{Na}_2\text{S}_2\text{O}_4$ solution (4 mL) was added and the mixture was stirred at rt for 10 min. The crude of reaction was concentrated under vacuum to remove THF and the residue was diluted with EtOAc (20 mL) and partitioned with saturated NaHCO_3 solution (3×10 mL). The organic layer was washed with brine solution and dried over Na_2SO_4 . After filtration, the solvent was evaporated under vacuum. The pure product 7 was obtained after column chromatography on Diol silica gel (100 \rightarrow 80:20 *n*-hexane/acetone) with 38% yield (22.3 mg). ^1H -NMR (500 MHz, CDCl_3): 7.12 (d, $J = 8.2$ Hz, 2 H, H-2B/H-6B), 6.83 (d, $J = 8.2$ Hz, 2 H, H-3B/H-5B), 6.77 (s, 1 H, H-5A), 6.69 (s, 1 H, H-2A), 5.15 (bs, 2 H, 3A-OH/4A-OH), 4.86 (bs, 1 H, 4B-OH), 2.41 (m, 2 H, CH_2 -7A), 1.44 (m, 2 H, CH_2 -8A), 0.79 (t, $J = 7.3$ Hz, 3 H, CH_3 -9A) ppm. ^{13}C -NMR (125 MHz, CDCl_3): 154.2 (C, C-4B), 142.5 (C, C-4A), 140.8 (C, C-3A), 134.2 (C, C-1B), 134.1 (C, C-1A), 133.3 (C, C-6A), 130.6 (CH, C-2B/C-6B), 117.1 (CH, C-2A), 116.0 (CH, C-5A), 114.8 (CH, C-3B/C-5B), 34.5 (CH_2 , C-7A), 24.6 (CH_2 , C-8A), 13.1 (CH_3 , C-9A) ppm. HRESIMS m/z 243.1049 [$\text{M}-\text{H}$] $^-$ (calcd for $\text{C}_{15}\text{H}_{12}\text{O}_3$, 243.2857).

3.3. Inhibited Autoxidation Studies

Autoxidation experiments were performed in a two-channel oxygen uptake apparatus, based on a Validyne DP 15 differential pressure transducer built in our laboratory [32]. The chain-breaking antioxidant activity of the title compounds was evaluated by studying the inhibition of the thermally initiated autoxidation of cumene (3.6 M) or styrene (4.3 M) in chlorobenzene and acetonitrile. In a typical experiment, an air-saturated mixture of the oxidizable substrate and the solvent, 1:1 (*v/v*) containing AIBN (0.05 M) as initiator was equilibrated with an identical reference solution containing an excess of PMHC so as to block any radical chain in the reference and avoid significant consumption of the antioxidant therein during the experiment. After equilibration, and when a constant O_2 consumption was reached, a concentrated solution of the antioxidant (final concentration = 5–20 μM) was injected in the sample flask. The oxygen consumption in the sample was measured after calibration of the apparatus from the differential pressure recorded with time between the two channels. Initiation rates, R_i , were determined for each condition in preliminary experiments by the inhibitor method using PMHC as a reference antioxidant: $R_i = 2[\text{PMHC}]/\tau$, where τ is the length of the induction period. PhCl/Cumene $R_i = 5.9 \times 10^{-9} \text{ Ms}^{-1}$; MeCN/Cumene $R_i = 8.2 \times 10^{-9} \text{ Ms}^{-1}$; PhCl /Styrene $R_i = 6.2 \times 10^{-9} \text{ Ms}^{-1}$. From the slope of oxygen consumption in the absence of antioxidant ($-d[\text{O}_2]/dt)_0 = R_{\text{ox}0}$) and during the inhibited period ($-d[\text{O}_2]/dt = R_{\text{ox}}$), k_{inh} values were obtained by using Equation (8). The $2k_t$ values of styrene and cumene at 303 K are 4.2×10^7 and $4.6 \times 10^4 \text{ M}^{-1}\text{s}^{-1}$, respectively [54,55].

3.4. Theoretical Calculations

Geometry optimizations and frequencies calculations were carried out at the B3LYP-D3/6-31+G(d,p) with implicit solvent chlorobenzene (SDM) using Gaussian 09 [52]. Stationary points and transition states were confirmed by checking the absence of imaginary frequencies. The BDE(OH) values were determined by the isodesmic approach, from the total energy in solution computed by single point calculations, and by applying thermal correction to enthalpy.

3.5. Statistical Analysis

Each value was taken from at least three independent measurements, and results are expressed as an average. Errors for n and k_{inh} represent \pm SD (SD = standard deviation).

4. Conclusions

In this work, the rate constants of the reaction of peroxy radicals ROO• with honokiol **1**, its two derivatives **2** and **3**, and the other four bisphenol neolignans **4–7** were determined in apolar and polar solvents. The different hydroxyl and alkyl substitutions on the phenolic skeleton of the synthesized compounds affects their antioxidant activity, compared to that of the natural derivative honokiol **1**. The presence of alkyl groups in the *ortho*-position with respect to the -OH groups decreases the k_{inh} as well as the presence of 2-hydroxyethyl substituents. 4,4'-dihydroxybiphenylic structures increase the overall inhibition constant compared with honokiol, but lead to a decrease in the number of trapped radicals ($n = 2$ vs. $n = 4$). Compounds showing quinone-like oxidized forms (e.g., **1ox**, **5ox** and **7ox**) can be regenerated by exploiting the reducing effect of hydroperoxy radicals generated by the addition of 1,4-cyclohexadiene to the reaction environment. This synergy occurs due to a catalytic cycle in which CHD acts as the sacrificial reductant, releasing HOO• radicals during the autoxidation and the consequent chain-transfer processes. For such quinones, the obtained antioxidant effect is enhanced if combined with HOO• radicals, rather than that of the starting compounds. The superior radical trapping activity of catechol derivative **7** and its ability to be regenerated by HOO• renders it an interesting molecule for further bioactivity studies.

Hopefully, the data presented herein will aid future investigation in the area, including the rational design of novel bioactive structures and possibly pharmacologically active lignans.

Supplementary Materials: The following supporting information can be downloaded at: <https://www.mdpi.com/article/10.3390/molecules28020735/s1>, Figure S1: biosynthetic pathway for phenyl propanoids, lignans and neolignans [56]; Figures S2–S5: NMR analysis of compound **7**.

Author Contributions: Conceptualization, A.B., V.M. and R.A.; methodology, N.C., V.M., R.A. and A.B.; software, R.A. and F.M.; validation, A.B. and R.A.; formal analysis, N.C. and F.M.; investigation, N.C. and A.B.; resources, V.M.; data curation, V.M. and A.B.; writing—original draft preparation, A.B., N.C., V.M. and R.A.; writing—review and editing, A.B., N.C., V.M. and R.A.; supervision, V.M. and R.A.; funding acquisition, V.M. All authors have read and agreed to the published version of the manuscript.

Funding: This research was funded by MUR ITALY PRIN 2017, grant number No. 2017A95NCJ.

Institutional Review Board Statement: Not applicable.

Informed Consent Statement: Not applicable.

Data Availability Statement: The data presented in this study are available on request from the corresponding author.

Acknowledgments: This research was supported by the Italian Ministry of Research (MUR) and by the CNR (Progetto PHEEL).

Conflicts of Interest: The authors declare no conflict of interest.

Sample Availability: Samples of the compounds are available from the authors.

References

1. Bernini, R.; Gualandi, G.; Crestini, C.; Barontini, M.; Belfiore, M.C.; Willfor, S.; Eklund, P.; Saladino, R. A novel and efficient synthesis of highly oxidized lignans by a methyltrioxorhenium/hydrogen peroxide catalytic system. Studies on their apoptogenic and antioxidant activity. *Bioorg. Med. Chem.* **2009**, *17*, 5676–5682. [CrossRef] [PubMed]
2. Aldemir, H.; Richarz, R.; Gulder, T.A. The biocatalytic repertoire of natural biaryl formation. *Angew. Chem. Int. Ed.* **2014**, *53*, 8286–8293. [CrossRef] [PubMed]

3. Cardullo, N.; Muccilli, V.; Tringali, C. Laccase-mediated synthesis of bioactive natural products and their analogues. *RSC Chem. Biol.* **2022**, *3*, 614–647. [[CrossRef](#)]
4. Teponno, R.B.; Kusari, S.; Spitteller, M. Recent advances in research on lignans and neolignans. *Nat. Prod. Rep.* **2016**, *33*, 1044–1092. [[CrossRef](#)]
5. Zalesak, F.; Bon, D.J.D.; Pospisil, J. Lignans and Neolignans: Plant secondary metabolites as a reservoir of biologically active substances. *Pharmacol. Res.* **2019**, *146*, 104284. [[CrossRef](#)]
6. López-Biedma, A.; Sánchez-Quesada, C.; Delgado-Rodríguez, M.; Gaforio, J.J. The biological activities of natural lignans from olives and virgin olive oils: A review. *J. Funct. Foods* **2016**, *26*, 36–47. [[CrossRef](#)]
7. Schuster, C.; Wolpert, N.; Moustaid-Moussa, N.; Gollahon, L.S. Combinatorial Effects of the Natural Products Arctigenin, Chlorogenic Acid, and Cinnamaldehyde Commit Oxidation Assassination on Breast Cancer Cells. *Antioxidants* **2022**, *11*, 591. [[CrossRef](#)]
8. Xu, Y.; Li, L.-Z.; Cong, Q.; Wang, W.; Qi, X.-L.; Peng, Y.; Song, S.-J. Bioactive lignans and flavones with in vitro antioxidant and neuroprotective properties from *Rubus idaeus* rhizome. *J. Funct. Foods* **2017**, *32*, 160–169. [[CrossRef](#)]
9. Di Micco, S.; Spatafora, C.; Cardullo, N.; Riccio, R.; Fischer, K.; Pergola, C.; Koeberle, A.; Werz, O.; Chalal, M.; Vervandier-Fasseur, D.; et al. 2,3-Dihydrobenzofuran privileged structures as new bioinspired lead compounds for the design of mPGES-1 inhibitors. *Bioorg. Med. Chem.* **2016**, *24*, 820–826. [[CrossRef](#)]
10. Hajduk, P.J.; Bures, M.; Praestgaard, J.; Fesik, S.W. Privileged molecules for protein binding identified from NMR-based screening. *J. Med. Chem.* **2000**, *43*, 3443–3447. [[CrossRef](#)]
11. Lee, Y.J.; Lee, Y.M.; Lee, C.K.; Jung, J.K.; Han, S.B.; Hong, J.T. Therapeutic applications of compounds in the *Magnolia* family. *Pharmacol. Ther.* **2011**, *130*, 157–176. [[CrossRef](#)]
12. Chen, J.H.; Kuo, H.C.; Lee, K.F.; Tsai, T.H. Magnolol protects neurons against ischemia injury via the downregulation of p38/MAPK, CHOP and nitrotyrosine. *Toxicol. Appl. Pharmacol.* **2014**, *279*, 294–302. [[CrossRef](#)] [[PubMed](#)]
13. Li, J.; Meng, A.P.; Guan, X.L.; Li, J.; Wu, Q.; Deng, S.P.; Su, X.J.; Yang, R.Y. Anti-hepatitis B virus lignans from the root of *Streblus asper*. *Bioorg. Med. Chem. Lett.* **2013**, *23*, 2238–2244. [[CrossRef](#)] [[PubMed](#)]
14. Kuo, D.H.; Lai, Y.S.; Lo, C.Y.; Cheng, A.C.; Wu, H.; Pan, M.H. Inhibitory effect of magnolol on TPA-induced skin inflammation and tumor promotion in mice. *J. Agric. Food. Chem.* **2010**, *58*, 5777–5783. [[CrossRef](#)] [[PubMed](#)]
15. Hsiao, C.H.; Yao, C.J.; Lai, G.M.; Lee, L.M.; Whang-Peng, J.; Shih, P.H. Honokiol induces apoptotic cell death by oxidative burst and mitochondrial hyperpolarization of bladder cancer cells. *Exp. Ther. Med.* **2019**, *17*, 4213–4222. [[CrossRef](#)]
16. Pulvirenti, L.; Muccilli, V.; Cardullo, N.; Spatafora, C.; Tringali, C. Chemoenzymatic Synthesis and alpha-Glucosidase Inhibitory Activity of Dimeric Neolignans Inspired by Magnolol. *J. Nat. Prod.* **2017**, *80*, 1648–1657. [[CrossRef](#)]
17. Cassiano, C.; Esposito, R.; Tosco, A.; Casapullo, A.; Mozzicafreddo, M.; Tringali, C.; Riccio, R.; Monti, M.C. Chemical Proteomics-Guided Identification of a Novel Biological Target of the Bioactive Neolignan Magnolol. *Front. Chem.* **2019**, *7*, 53. [[CrossRef](#)]
18. Maioli, M.; Basoli, V.; Carta, P.; Fabbri, D.; Dettori, M.A.; Cruciani, S.; Serra, P.A.; Delogu, G. Synthesis of magnolol and honokiol derivatives and their effect against hepatocarcinoma cells. *PLoS ONE* **2018**, *13*, e0192178. [[CrossRef](#)]
19. Fuchs, A.; Baur, R.; Schoeder, C.; Sigel, E.; Muller, C.E. Structural analogues of the natural products magnolol and honokiol as potent allosteric potentiators of GABA(A) receptors. *Bioorg. Med. Chem.* **2014**, *22*, 6908–6917. [[CrossRef](#)]
20. Chu, J.; Yang, R.; Cheng, W.; Cui, L.; Pan, H.; Liu, J.; Guo, Y. Semisynthesis, biological activities, and mechanism studies of Mannich base analogues of magnolol/honokiol as potential alpha-glucosidase inhibitors. *Bioorg. Med. Chem.* **2022**, *75*, 117070. [[CrossRef](#)]
21. Fried, L.E.; Arbiser, J.L. Honokiol, a multifunctional antiangiogenic and antitumor agent. *Antioxid. Redox Signal.* **2009**, *11*, 1139–1148. [[CrossRef](#)] [[PubMed](#)]
22. Zhao, C.; Liu, Z.Q. Comparison of antioxidant abilities of magnolol and honokiol to scavenge radicals and to protect DNA. *Biochimie* **2011**, *93*, 1755–1760. [[CrossRef](#)] [[PubMed](#)]
23. Amorati, R.; Zotova, J.; Baschieri, A.; Valgimigli, L. Antioxidant Activity of Magnolol and Honokiol: Kinetic and Mechanistic Investigations of Their Reaction with Peroxyl Radicals. *J. Org. Chem.* **2015**, *80*, 10651–10659. [[CrossRef](#)] [[PubMed](#)]
24. Helberg, J.; Pratt, D.A. Autoxidation vs. antioxidants—the fight for forever. *Chem. Soc. Rev.* **2021**, *50*, 7343–7358. [[CrossRef](#)] [[PubMed](#)]
25. Shah, R.; Farmer, L.A.; Zilka, O.; Van Kessel, A.T.M.; Pratt, D.A. Beyond DPPH: Use of Fluorescence-Enabled Inhibited Autoxidation to Predict Oxidative Cell Death Rescue. *Cell Chem. Biol.* **2019**, *26*, 1594–1607.e7. [[CrossRef](#)] [[PubMed](#)]
26. Baschieri, A.; Pulvirenti, L.; Muccilli, V.; Amorati, R.; Tringali, C. Chain-breaking antioxidant activity of hydroxylated and methoxylated magnolol derivatives: The role of H-bonds. *Org. Biomol. Chem.* **2017**, *15*, 6177–6184. [[CrossRef](#)]
27. Baschieri, A.; Amorati, R. Methods to Determine Chain-Breaking Antioxidant Activity of Nanomaterials beyond DPPH(*). A Review. *Antioxidants* **2021**, *10*, 1551. [[CrossRef](#)]
28. Cardullo, N.; Barresi, V.; Muccilli, V.; Spampinato, G.; D’Amico, M.; Condorelli, D.F.; Tringali, C. Synthesis of Bisphenol Neolignans Inspired by Honokiol as Antiproliferative Agents. *Molecules* **2020**, *25*, 733. [[CrossRef](#)]
29. Bizzarri, B.M.; Botta, L.; Capocchi, E.; Celestino, I.; Checconi, P.; Palamara, A.T.; Nencioni, L.; Saladino, R. Regioselective IBX-Mediated Synthesis of Coumarin Derivatives with Antioxidant and Anti-influenza Activities. *J. Nat. Prod.* **2017**, *80*, 3247–3254. [[CrossRef](#)]

30. Frigerio, M.; Santagostino, M.; Sputore, S. A User-Friendly Entry to 2-Iodoxybenzoic Acid (IBX). *J. Org. Chem.* **1999**, *64*, 4537–4538. [[CrossRef](#)]
31. Burton, G.W.; Doba, T.; Gabe, E.; Hughes, L.; Lee, F.L.; Prasad, L.; Ingold, K.U. Autoxidation of biological molecules. 4. Maximizing the antioxidant activity of phenols. *J. Am. Chem. Soc.* **1985**, *107*, 7053–7065. [[CrossRef](#)]
32. Amorati, R.; Baschieri, A.; Valgimigli, L. Measuring Antioxidant Activity in Bioorganic Samples by the Differential Oxygen Uptake Apparatus: Recent Advances. *J. Chem.* **2017**, *2017*, 1–12. [[CrossRef](#)]
33. Amorati, R.; Pedulli, G.F.; Valgimigli, L.; Attanasi, O.A.; Filippone, P.; Fiorucci, C.; Saladino, R. Absolute rate constants for the reaction of peroxy radicals with cardanol derivatives. *J. Chem. Soc., Perkin Trans. II* **2001**, *2*, 2142–2146. [[CrossRef](#)]
34. Chatgililoglu, C.; Timokhin, V.I.; Zaborovskiy, A.B.; Lutsyk, D.S.; Prystansky, R.E. Rate constants for the reaction of cumylperoxy radicals with group 14 hydrides. *J. Chem. Soc., Perkin Trans. II* **2000**, 577–582. [[CrossRef](#)]
35. Denisov, E.T.; Khudyakov, I.V. Mechanisms of action and reactivities of the free radicals of inhibitors. *Chem. Rev.* **2002**, *87*, 1313–1357. [[CrossRef](#)]
36. Denisov, E.T. *Liquid-Phase Reaction Rate Constants*; Springer: New York, NY, USA, 1995.
37. Lucarini, M.; Pedulli, G.F.; Valgimigli, L.; Amorati, R.; Minisci, F. Thermochemical and Kinetic Studies of a Bisphenol Antioxidant. *J. Org. Chem.* **2001**, *66*, 5456–5462. [[CrossRef](#)]
38. Amorati, R.; Lucarini, M.; Mugnaini, V.; Pedulli, G.F. Antioxidant activity of o-bisphenols: The role of intramolecular hydrogen bonding. *J. Org. Chem.* **2003**, *68*, 5198–5204. [[CrossRef](#)]
39. Valgimigli, L.; Pratt, D.A. Antioxidants in Chemistry and Biology. In *Encyclopedia of Radicals in Chemistry, Biology and Materials*; Wiley: Hoboken, NJ, USA, 2012.
40. Amorati, R.; Baschieri, A.; Morroni, G.; Gambino, R.; Valgimigli, L. Peroxyl Radical Reactions in Water Solution: A Gym for Proton-Coupled Electron-Transfer Theories. *Chem. Eur. J.* **2016**, *22*, 7924–7934. [[CrossRef](#)]
41. Foti, M.C.; Barclay, L.R.; Ingold, K.U. The role of hydrogen bonding on the h-atom-donating abilities of catechols and naphthalene diols and on a previously overlooked aspect of their infrared spectra. *J. Am. Chem. Soc.* **2002**, *124*, 12881–12888. [[CrossRef](#)]
42. Howard, J.A.; Ingold, K.U. Absolute rate constants for hydrocarbon autoxidation. V. The hydroperoxy radical in chain propagation and termination. *Can. J. Chem.* **1967**, *45*, 785–792. [[CrossRef](#)]
43. Sawyer, D.T.; McDowell, M.S.; Yamaguchi, K.S. Reactivity of perhydroxyl (HOO•) with 1,4-cyclohexadiene (model for allylic groups in biomembranes). *Chem. Res. Toxicol.* **1988**, *1*, 97–100. [[CrossRef](#)] [[PubMed](#)]
44. Baschieri, A.; Amorati, R.; Valgimigli, L.; Sambri, L. 1-Methyl-1,4-cyclohexadiene as a Traceless Reducing Agent for the Synthesis of Catechols and Hydroquinones. *J. Org. Chem.* **2019**, *84*, 13655–13664. [[CrossRef](#)] [[PubMed](#)]
45. Baschieri, A.; Valgimigli, L.; Gabbanini, S.; DiLabio, G.A.; Romero-Montalvo, E.; Amorati, R. Extremely Fast Hydrogen Atom Transfer between Nitroxides and HOO• Radicals and Implication for Catalytic Coantioxidant Systems. *J. Am. Chem. Soc.* **2018**, *140*, 10354–10362. [[CrossRef](#)] [[PubMed](#)]
46. Guo, Y.; Baschieri, A.; Mollica, F.; Valgimigli, L.; Cedrowski, J.; Litwinienko, G.; Amorati, R. Hydrogen Atom Transfer from HOO• to ortho-Quinones Explains the Antioxidant Activity of Polydopamine. *Angew. Chem. Int. Ed.* **2021**, *60*, 15220–15224. [[CrossRef](#)]
47. Becke, A.D. Density-functional thermochemistry. III. The role of exact exchange. *J. Chem. Phys.* **1993**, *98*, 5648–5652. [[CrossRef](#)]
48. Lee, C.; Yang, W.; Parr, R.G. Development of the Colle-Salvetti correlation-energy formula into a functional of the electron density. *Phys. Rev. B Condens. Matter.* **1988**, *37*, 785–789. [[CrossRef](#)]
49. Grimme, S.; Antony, J.; Ehrlich, S.; Krieg, H. A consistent and accurate ab initio parametrization of density functional dispersion correction (DFT-D) for the 94 elements H-Pu. *J. Chem. Phys.* **2010**, *132*, 154104. [[CrossRef](#)]
50. Grimme, S.; Ehrlich, S.; Goerigk, L. Effect of the damping function in dispersion corrected density functional theory. *J. Comput. Chem.* **2011**, *32*, 1456–1465. [[CrossRef](#)]
51. Marenich, A.V.; Cramer, C.J.; Truhlar, D.G. Universal solvation model based on solute electron density and on a continuum model of the solvent defined by the bulk dielectric constant and atomic surface tensions. *J. Phys. Chem. B* **2009**, *113*, 6378–6396. [[CrossRef](#)]
52. Frisch, M.J.; Trucks, G.W.; Schlegel, H.B.; Scuseria, G.E.; Robb, M.A.; Cheeseman, J.R.; Scalmani, G.; Barone, V.; Mennucci, B.; Petersson, G.A.; et al. *Gaussian 09, Revision D.01*; Gaussian, Inc.: Wallingford, CT, USA, 2009.
53. Valgimigli, L.; Amorati, R.; Fumo, M.G.; DiLabio, G.A.; Pedulli, G.F.; Ingold, K.U.; Pratt, D.A. The unusual reaction of semiquinone radicals with molecular oxygen. *J. Org. Chem.* **2008**, *73*, 1830–1841. [[CrossRef](#)]
54. Howard, J.A.; Ingold, K.U. Absolute rate constants for hydrocarbon autoxidation. VI. Alkyl aromatic and olefinic hydrocarbons. *Can. J. Chem.* **1967**, *45*, 793–802. [[CrossRef](#)]
55. Enes, R.F.; Tome, A.C.; Cavaleiro, J.A.; Amorati, R.; Fumo, M.G.; Pedulli, G.F.; Valgimigli, L. Synthesis and antioxidant activity of [60]fullerene-BHT conjugates. *Chem. Eur. J.* **2006**, *12*, 4646–4653. [[CrossRef](#)] [[PubMed](#)]
56. Dewick, P.M. The shikimate pathway: Aromatic amino acids and phenylpropanoids. In *Medicinal Natural Products: A Biosynthetic Approach*, 3rd ed.; John Wiley & Sons Ltd.: Hoboken, NJ, USA, 2009; pp. 137–186. [[CrossRef](#)]

Disclaimer/Publisher's Note: The statements, opinions and data contained in all publications are solely those of the individual author(s) and contributor(s) and not of MDPI and/or the editor(s). MDPI and/or the editor(s) disclaim responsibility for any injury to people or property resulting from any ideas, methods, instructions or products referred to in the content.